Alzheimer's Disease : Diagnosis by Different Methods of Voxel-Based Morphometry

Dashjamts, Tuvshinjargal
Departments of Clinical Radiology, Graduate School of Medical Sciences, Kyushu University

Yoshiura, Takashi
Departments of Clinical Radiology, Graduate School of Medical Sciences, Kyushu University

Hiwatashi, Akio
Departments of Clinical Radiology, Graduate School of Medical Sciences, Kyushu University

Togao, Osamu
Departments of Clinical Radiology, Graduate School of Medical Sciences, Kyushu University

他

https://doi.org/10.15017/21752

出版情報：福岡醫學雜誌. 103 (3), pp.59-69, 2012-03-25. 福岡医学会
バージョン：
権利関係：

Original Article

Alzheimer's Disease: Diagnosis by Different Methods of Voxel-Based Morphometry

Tuvshinjargal Dashjamts[1)], Takashi Yoshiura[1)], Akio Hiwatashi[1)], Osamu Togao[1)], Koji Yamashita[1)], Yasumasa Ohyagi[2)], Akira Monji[3)], Hironori Kamano[1)], Toshiro Kawashima[3)], Jun-ichi Kira[2)] and Hiroshi Honda[1)]

Departments of [1)]Clinical Radiology, [2)]Neurology and [3)]Neuropsychiatry, Graduate School of Medical Sciences, Kyushu University, Fukuoka, Japan

Abstract　*Purpose* : The purpose of this study was to determine the optimal computational options in voxel-based morphometry (VBM) for discrimination between Alzheimer's disease (AD) patients and healthy control (HC) subjects.
Materials and Methods : Structural magnetic resonance images of 24 AD patients and 26 HC subjects were analyzed using VBM to determine brain regions with significant gray matter (GM) loss due to AD. The VBM analyses were performed with 4 different computational options : gray matter concentration (GMC) analysis with and without global normalization, and gray matter volume (GMV) analysis, with and without global normalization. Statistical maps calculated with the 4 computational options were obtained at 3 different P-value thresholds ($P < 0.001$, $P < 0.0005$, and $P < 0.0001$, uncorrected for multiple comparisons), yielding a total of 12 sets of maps, from which regions-of-interest (ROI) were generated for subsequent analyses of performance in terms of discrimination between AD patients and HC subjects as based on the mean value of either the GMC or GMV within the ROI for each of the 12 maps. Discrimination performance was evaluated by means of comparing the area-under-the-curve derived from the receiver-operating characteristic analysis as well as on the accuracy of the discrimination.
Results : Discrimination based on GMC analysis resulted in better performance than that based on GMV analysis. The best discrimination performance was achieved with GMC analysis either with or without proportional global normalization.
Conclusion : The findings suggested that GMC-based VBM is better suited than GMV-based VBM for discrimination between AD patients and HC subjects.

Key words : MRI, Alzheimer's disease, Voxel-based morphometry

Introduction

In the majority of developed countries, Alzheimer's disease (AD) is the most common progressive illness leading to dementia[1)~3)]. Although in the clinical practice, the role played by structural magnetic resonance (MR) imaging of the brain has been confined primarily to ruling out alternative causes of dementia, MR imaging has been increasingly recognized as a tool for the early diagnosis of AD. With the advent of new therapeutic agents, such as cholinesterase-inhibitors, which have been shown to be efficacious in the early AD stages[4)~6)], the identification of AD-compatible morphological features prior to the onset of severe clinical dementia is a crucial component of clinical decision-making and is relevant for the assessment of promising therapies in the context of clinical trials[7)]. Fully

Corresponding author :
Takashi Yoshiura, MD, PhD
Department of Clinical Radiology, Graduate School of Medical Sciences, Kyushu University
3-1-1 Maidashi, Higashi-ku, Fukuoka 812-8582, Japan
Phone : + 81-92-642-5695 ; Fax : + 81-92-642-5708
E-mail : tyoshiu@radiol.med.kyushu-u.ac.jp

automated voxel-based morphometry (VBM)[8] objectively detects disease-related alterations in regional brain tissue morphology and offers independence from the expertise of individual neuroradiologists. VBM has been used for group-wise studies of AD, as well as for distinguishing between individuals with AD from those without[9)~12)]. Recently, VBM was adopted into a dedicated software package for AD screening[11]. VBM consists of several steps of image processing, each of which has different computational options that may critically affect the final diagnostic results. Scarce number of publications on the assessment of the effects of variations in image processing as well as the divergent manner of reporting VBM results and the differences between applied VBM protocols make the tracing of such effects difficult and render it necessary to systematically evaluate VBM performance. The purpose of this study was to determine the optimal computational options in VBM for discrimination between AD patients and healthy control (HC) subjects.

Materials and Methods

The study was approved by the regional institutional review board, and informed consent was obtained from each HC subject. Clinical and imaging data for the AD patients were reviewed retrospectively, and the need to obtain informed consent was waived.

Subjects

Among those who visited the memory clinic at our hospital, 83 consecutive patients were identified respectively. Among these patients, those, who fulfilled the clinical criteria for AD were considered for inclusion in the study population. Each patient was diagnosed based on case conferences by both experienced neurologists and psychiatrists at our hospital, according to the criteria of the National Institute of Neurological and Communicative Disorders and Stroke, in concert with the criteria defined by the Alzheimer's Disease and Related Disorders Association[13] and the Diagnostic and Statistical Manual of Mental Disorders, 4th edition[14]. All patients received the Japanese version of the Mini-Mental Scale Examination (MMSE) test[15]. The interval between MMSE test and MR imaging ranged from 0 to 53 days (mean 26 days). Additionally, Raven's Colored Progressive Matrices and the Miyake's paired verbal associate learning test were routinely performed. During the diagnosis, both structural MR imaging results and single-photon emission tomography (SPECT) findings were taken into consideration. In addition, MR imaging was used to carefully exclude vascular dementia, according to the criteria of the National Institute of Neurological and Communicative Disorders and Stroke - Association Internationale pour la Recherche et l'Enseignement en Neuroscience[16]. All MR images of the patients were screened by a board-certified radiologist (T. Y.). Patients with a space-occupying lesion were excluded, since VBM has not been validated under such conditions. In addition, patients were excluded when artifacts degraded their MR images. Twenty-four patients (10 men and 14 women ; mean age ± SD, 74.4 ± 8.9 years) met the inclusion/exclusion criteria, and were included in this study. The MMSE scores of these patients ranged from 11 to 29 (mean ± SD = 21.2 ± 4.3).

The HC subjects were recruited from the general population. They had no history of hypertension, diabetes mellitus, cardiovascular disease, stroke, brain tumor, epilepsy, Parkinson's disease, dementia, depression, drug abuse, or head trauma. These candidate control subjects also received the MMSE. Only those recruited subjects who achieved 27 points or more were included in the study. The HC subjects were also assessed using the self-rating depression scale[17] in order to screen for depression, and those who scored 40 points or more were excluded from the present study. Twenty-six HC subjects (12 men and 14 women; mean age ±

SD, 73.6 ± 6.8 years; mean MMSE score ± SD, 29.4 ± 0.9) were included in the study.

MR imaging procedures

All images were acquired using a 3T MR imager (Achieva Quasar Dual ; Philips Medical Systems, Best, Netherlands) and an 8-channel head array coil. High-resolution T1-weighted images for morphological analysis were obtained using the following settings for three-dimensional (3D) magnetization-prepared rapid gradient-echo (MPRAGE) : repetition time = 8.3 ms, echo time = 3.8 ms, inversion time = 240 ms, flip angle = 8°, sensitivity encoding factor = 2, number of signal-intensity acquisitions = 1, field of view = 240 mm, matrix size = 240 × 240, slice thickness = 1 mm, imaging time = 5 min 20 s. The images were reconstructed into 1-mm-thick consecutive transverse images.

Image analysis

VBM analysis was performed using SPM8 software (Welcome Trust Center for Neuroimaging, London, UK, http://www.fil.ion.ucl.ac.uk/spm/software/spm8/). The images were segmented into gray matter (GM) and white matter (WM) images. Next, roughly aligned isotropic (1.5x1.5x1.5 mm^3) GM images were obtained such that the images could be imported for subsequent non-linear registration based on an algorithm referred to as "diffeomorphic anatomical registration through exponentiated lie algebra" (DARTEL)[18]. The GM images of all subjects were non-linearly registered to the "template" images, which were initially created by averaging GM images from all subjects, i.e. all HC subjects and AD patients. The GM images of each subject registered to the template by iterative calculations were spatially normalized into a common stereotactic space. Finally, the images were smoothed using an 8 mm full-width-at-half-maximum isotropic 3D Gaussian kernel. For each subject, we prepared two sets of GM images, including those obtained with and without "modulation", which was applied to correct for volume alterations due to deformation during spatial normalization[19]. Specifically, such modulation involves multiplying voxel values by the Jacobian determinants derived from the spatial normalization step. In images obtained without the modulation, the value of each voxel represents the local GM concentration (GMC), whereas it represents the local GM volume (GMV) in images obtained with the modulation. In

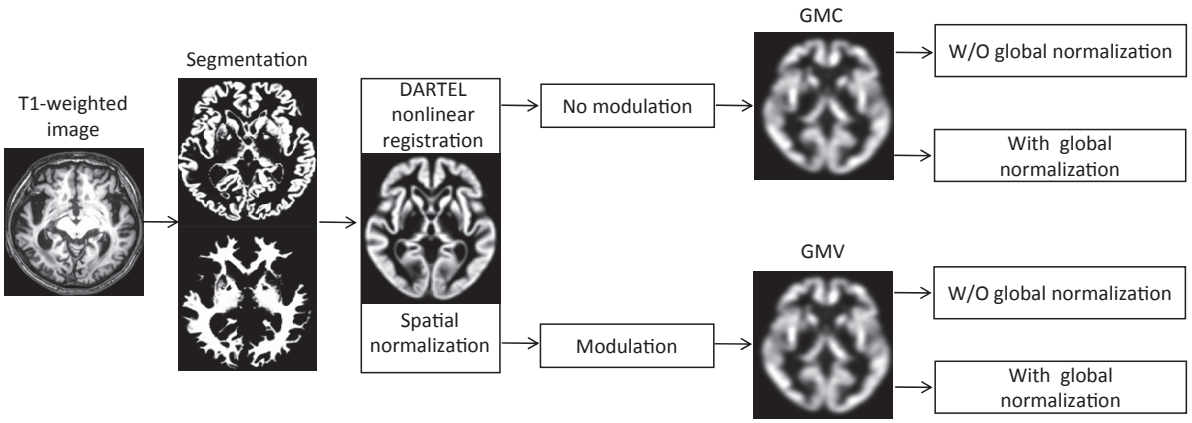

Fig. 1 Voxel-based morphometric (VBM) analysis of structural magnetic resonance images. T1-weighted images of each subject were first segmented into gray matter (GM) and white matter images. The GM images were then spatially normalized using a non-linear registration algorithm rendering to as "diffeomorphic anatomical registration through exponentiated lie algebra" (DARTEL). The voxel values of the spatially normalized GM image represent the local gray matter concentration (GMC). By applying a modulation to the spatially normalized GM image, the voxel values represent the local gray matter volume (GMV). For both GMC and GMV images, there was the option of either using or not using proportional global normalization. Thus, there were 4 different computational options in the VBM analysis.

addition, for both GMC images and GMV images, there was another option of performing the analysis either with or without proportional global normalization to control for individual variation in the global mean, where the value of each voxel was normalized by the proportional scaling to the global mean value. Thus, there were 4 different computational options in the VBM analysis (Fig 1).

Statistical analysis

A two-sample t-test was conducting using SPM8 to determine areas with significantly reduced GMC or GMV in AD patients as compared to HC subjects. Absolute threshold masking was employed to exclude voxels outside of GM regions. The statistical maps were generated at different voxel-wise significance levels of $P < 0.001$, $P < 0.0005$, and $P < 0.0001$, uncorrected for multiple comparisons. Finally, we generated 12 sets of statistical maps, including those for GMC and GMV obtained with and without global normalization at 3 different P value thresholds. Each of the 12 statistical maps was binarized and was used as a region-of-interest (ROI) in the subsequent analysis of the discrimination performance.

Discrimination between AD patients and HC subjects was attempted based on the mean values of either the GMC or GMV within the ROI generated from each of the 12 statistical maps in the previous step. The discrimination performance of each approach was evaluated by the area-under-the-curve (AUC) values derived from the receiver-operating characteristic (ROC) analysis using ROCKIT 1.1 B2 software (Kurt Rossmann Laboratories for Radiologic Image Research, The University of Chicago, Chicago, IL, USA), as well as from the sensitivity, specificity, positive predictive value, negative predictive value, and accuracy of the discrimination calculated using the linear discriminant analysis on JMP8.0 (SAS Institute, Cary, NC, USA).

Results

VBM analysis

The results of the VBM analyses of GMC with and without the proportional global normalization at three different P-value threshold settings ($P < 0.001$, $P < 0.0005$, and $P < 0.0001$, uncorrected for multiple comparisons, respectively) are shown in Fig. 2. Comparison of the GMC without global normalization revealed areas of significant GM loss due to AD which were distributed in a scattered pattern in both cerebral and cerebellar hemispheres with t-value peaks in the bilateral hippocampi (Fig. 2a). When proportional global normalization was added to the analysis, the areas of significant GM loss due to AD were reduced to areas of the bilateral hippocampi, bilateral temporal lobes, bilateral frontal lobes, right anterior insula and left inferior parietal lobule (Fig. 2b).

Figure 3 shows the results for the GMV analysis. In general, the areas of significant GMV loss due to AD were found to be more localized than the areas of significant GMC loss obtained at the same P-value thresholds as those shown in Fig 2. The areas of significant GMV loss were distributed in the bilateral hippocampi, right medial temporal lobe, right orbitofrontal region and left inferior parietal lobules (Fig. 3a). As seen in the GMC results, the inclusion of proportional global normalization resulted in a reduction in areas revealing significant differences (Fig 3b).

Analysis of discrimination performance

The results of the discrimination performance evaluation are summarized in Table 1. In general, discrimination based on GMC analysis (AUC range, 0.716-0.817) tended to be associated with better performance than that based on GMV analysis (AUC range, 0.624-0.745). The best discrimination performance was achieved either when the unmodulated data (GMC) were analyzed with proportional global normalization at a threshold of $P < 0.0005$ (AUC = 0.816, accuracy =

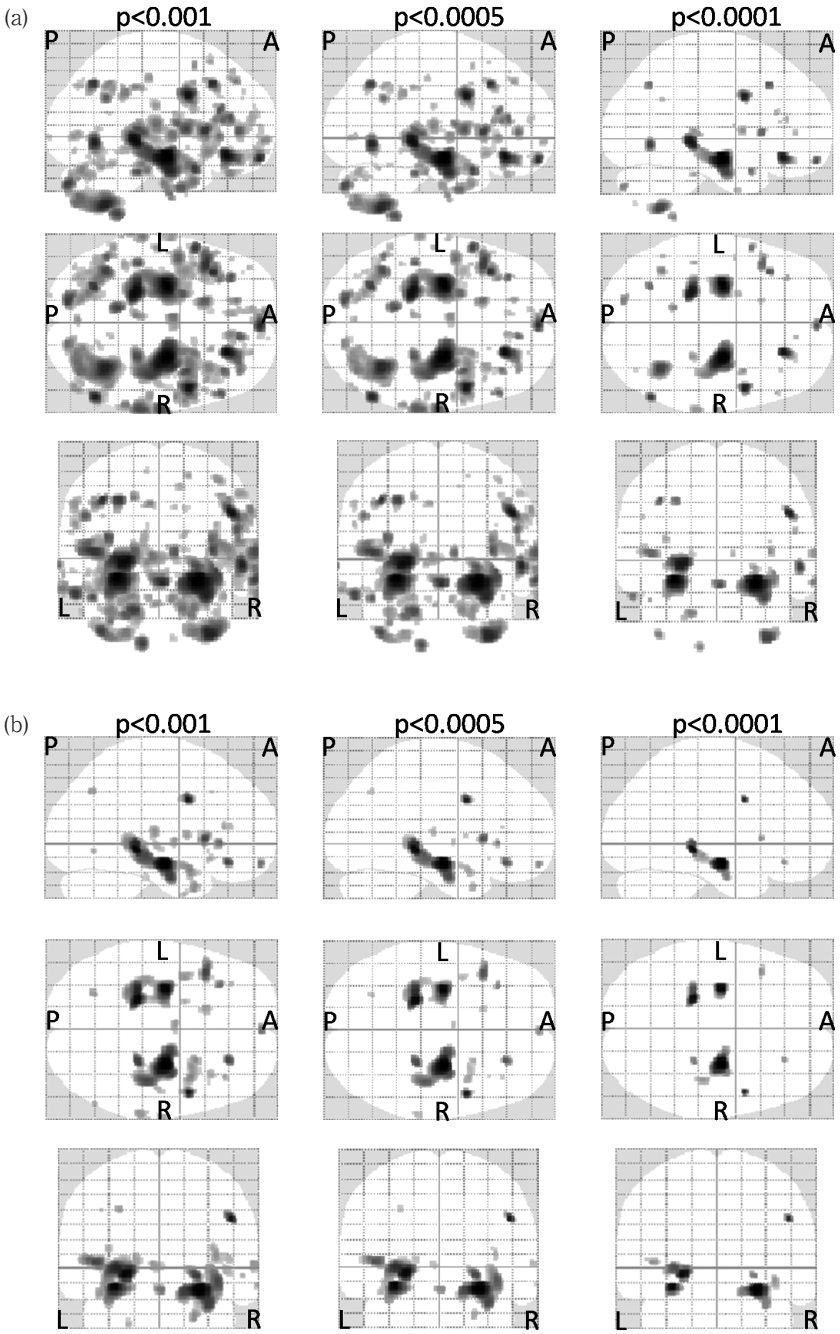

Fig. 2 Results of the group-wise VBM analysis of GMC obtained without (a) and with (b) proportional global normalization at three different P-value threshold settings ($P < 0.001$, $P < 0.0005$, and $P < 0.0001$, uncorrected for multiple comparisons). In each map, the gray scale reflects t value. P, posterior ; A, anterior ; L, left ; R, right.

80.0%), or when the GMC was analyzed without proportional global normalization at a threshold of $P < 0.0001$ (AUC = 0.817, accuracy = 74.0%) (Table 1).

Discussion

The present series demonstrated that the selection of different computational options for VBM gave different results, and the influence of the various options applied both to group comparisons and analyses of discrimination performance.

In both the GMC and GMV analyses, a significant loss of GM due to AD was consistently identified in the temporal lobe, including the

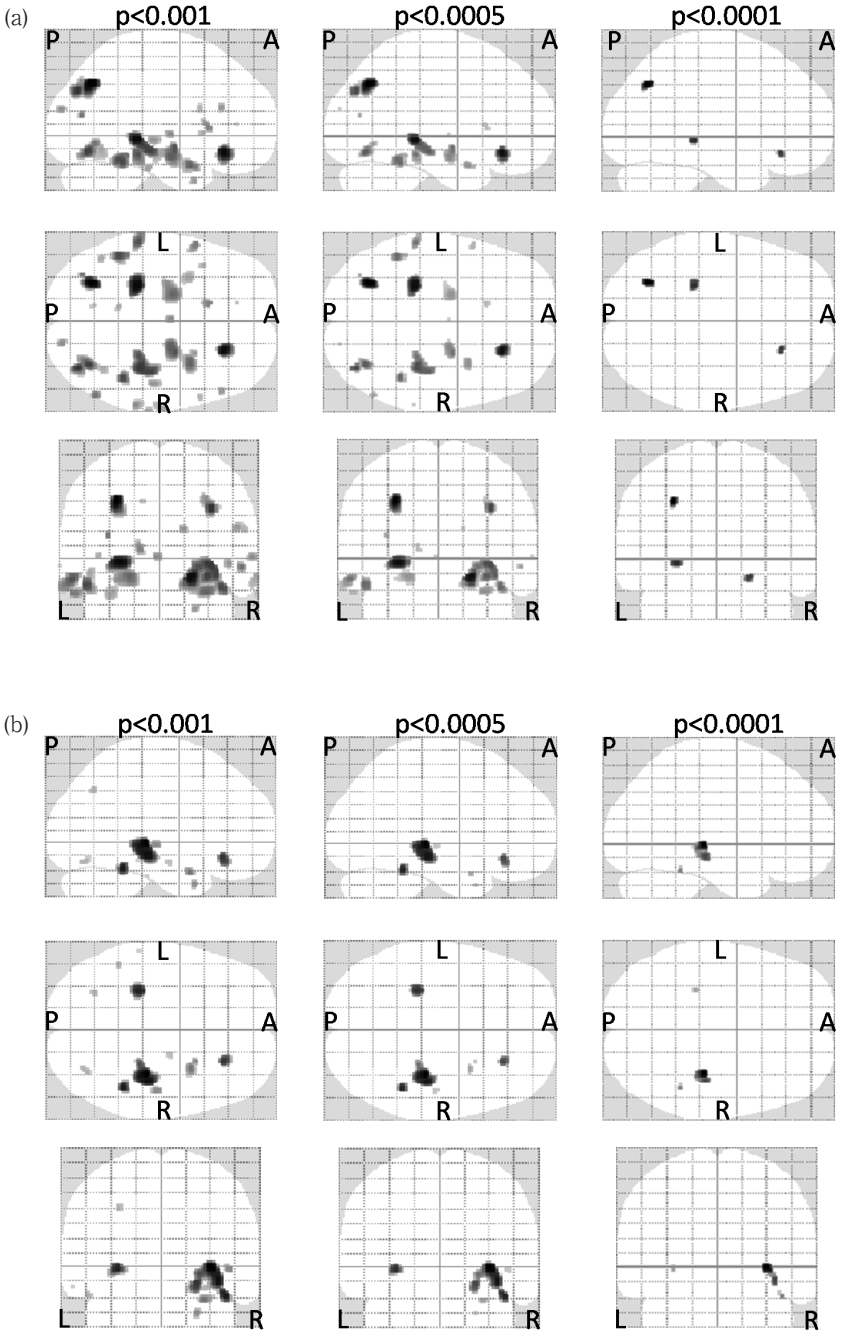

Fig. 3 Results of the group-wise VBM analysis of GMV obtained without (a) and with (b) proportional global normalization at three different P-value threshold settings ($P < 0.001$, $P < 0.0005$, and $P < 0.0001$, uncorrected for multiple comparisons). In each map, the gray scale reflects t value. P, posterior ; A, anterior ; L, left ; R, right.

hippocampus (Figs. 2 and 3). This finding was in agreement with those of previous morphometric studies[20)~26)] as well as with those of neuropathological studies[27)~29)]. On the other hand, a substantial difference was noted between the VBM results for the GMC and the GMV. In our study, at a given P-value threshold, the GMV analyses (Fig. 3) detected less extensive areas of significant GM loss than did the GMC analyses (Fig. 2). Such discrepant results in a group-wise comparison between GMC and GMV analyses have been reported frequently in studies of various neurological and neuropsychiatric diseases[30)~33)]. For example, a meta-analysis

Table 1 Analysis of discriminating performance

Gray matter measure	P-value	SE %	SP %	PPV %	NPV %	Accuracy	AUC
GMC W/O global normalization	< 0.001	54.1	69.2	61.9	62.1	62.0	0.716
	< 0.0005	58.3	73.1	66.7	65.5	66.0	0.744
	< 0.0001	66.7	80.8	76.2	72.4	74.0	0.817
GMC With global normalization	< 0.001	70.8	80.8	66.7	60.7	76.0	0.797
	< 0.0005	70.8	88.5	66.7	60.7	80.0	0.816
	< 0.0001	62.5	88.5	66.7	60.7	76.0	0.811
GMV W/O global normalization	< 0.001	62.5	73.1	68.2	67.9	68.0	0.729
	< 0.0005	62.5	76.9	71.4	69.0	70.0	0.745
	< 0.0001	58.3	65.4	60.9	63.0	62.0	0.624
GMV With global normalization	< 0.001	58.3	73.1	85.0	76.9	66.0	0.660
	< 0.0005	54.2	76.9	85.0	76.9	66.0	0.712
	< 0.0001	54.2	76.9	85.0	76.9	66.0	0.705

Note. GMC, gray matter concentration ; GMV, gray matter volume ; SE, sensitivity ; SP, specificity ; PPV, positive predicting values ; NPV, negative predicting value ; AUC, area-under-the-curve.

reported by Fortino *et al.*[33] describes such disagreement in schizophrenia studies, in which larger areas with GMC loss were distributed in a manner that differed areas showing GMV loss.

In the discrimination performance analysis, GMC-based discriminations tended to perform better than those based on GMV (Table 1). This tendency was consistent with that described in several previous reports. Wilke *et al.*[30] used the VBM to detect GM malformation, and their GMV analysis demonstrated lower detection sensitivity and identified smaller lesion volumes than did analysis of the GMC. A more recent publication by Bruggermann *et al.*[32] on the detection of dysplasia and neoplasia in childhood epilepsy showed greater sensitivity and specificity for GMC than GMV analysis. In the discrimination of AD patients from HC subjects, Matsunari *et al.*[34] used VBM, and they reported better performance with GMC (AUC = 0.832, accuracy = 85 %) compared to GMV (AUC = 0.782, accuracy = 79 %). It should be noted that all of these previous studies were based on older VBM regimens, i.e. either the so-called "classical" or "optimized" VBM. In our VBM analysis, the spatial normalization of the images was performed using the DARTEL algorithm, which is a more advanced and robust registration method compared to that used in either the classical or optimized VBM approach[35]. Our results suggest that the use of DARTEL registration does not change the advantage of GMC analysis over GMV analysis in terms of diagnostic performance.

The reason for the discrepant results between the GMC and GMV analyses remains unclear. Fortino *et al.*[33] raised the possibility that the modulation can increase inter-subject variability in the data. As noted earlier, the modulation is performed to correct for the volume alteration due to deformation during the spatial normalization. Since the modulation is dependent on the degree and nature of the deformation, it can introduce additional variability into the results, depending on the shape of the individual subject's brain, which may in turn reduce the statistical power of the analysis. In contrast, GMC analysis is conducted directly after spatial normalization, when the interindividual variability is minimized. Thus, GMC analysis may be more sensitive to systematic differences in the morphology of the local GM, while those "differences" may actually reflect alterations such as sulcal widening and displacement caused by AD pathology rather than true GM loss. It is conceivable that the better discrimination performance of the GMC analysis relative to that of the GMV analysis in this study (Table 1) was related to the greater sensitivity of the GMC analysis in the group

comparison.

As shown in Figs. 2 and 3, the use of proportional global normalization resulted in a more localized distribution of significant voxels within the medial temporal regions in both the GMC and GMV analyses. That finding is likely to have reflected a well-known distribution pattern for GM loss in AD patients, namely, rather than being diffusely distributed. GM loss in AD patients is limited to the medial temporal regions, especially during the early stages of disease[10)11)20)]. In the analysis of discrimination performance, the effect of proportional global normalization appears to be variable : in this series, global normalization appeared to have improved the performance in GMC analyses whereas no such effect was seen in the GMV analyses (Table 1). The underlying mechanism of this apparent differential effect of the global normalization on the discriminating performance of GMV and GMC analyses remains unexplained. This study has several limitations. The number of subjects included in the study was limited. In future studies, inclusion of a larger number of subjects will be desirable such that separate subject groups can be evaluated for the determination of discriminating criteria and the evaluation of overall performance. Although we found higher AUC values with GMC analysis than with GMV analysis (Table 1), we could not provide statistical significance for the differences of their AUC values due to the limited subject number. We used the DARTEL algorithm for spatial normalization, and we did not test older VBM regimens such as "classical" and "optimized" VBM. The effects of the normalization algorithm will still need to be clarified in future studies. In our study, discrimination was performed based on the averaged GMC/GMV within ROI. Averaged values were used in some previous reports[34)], while in other reports maximum Z-score within the ROI was used[11)]. We did not include the latter method. AD patients used in this study were on average relatively mild cases (mean MMSE score = 21.2). However, in clinical practice, diagnosis of even earlier AD or mild cognitive impairment is desirable. Further studies involving those patients are necessary.

Conclusion

We demonstrated that the choice of computational options in VBM can substantially affect both the results of group-wise comparisons as well as discrimination performance. Our findings suggested that VBM based on GMC analysis may be better suited for discrimination between AD patients and HC subjects than is VBM based on GMV analysis.

Acknowledgements

This study was supported in part by a grant-in-aid from the Japan Society for the Promotion of Science (No. 22591340) and by a grant-in-aid for Scientific Research on Innovative Areas (Comprehensive Brain Science Network) from the Ministry of Education, Culture, Sports, Science and Technology, Japan.

References

1) Wimo A and Prince M : World Alzheimer Report 2010 The global economic impact of Dementia. Alzheimer's Disease International ADI, London, 2010.
2) Matsui Y, Tanizaki Y, Arima H, Yonemoto K, Doi Y, Ninomiya T, Sasaki K, Iida M, Iwaki T, Kanba S and Kiyohara Y : Incidence and survival of dementia in a general population of Japanese elderly : the Hisayama study. J Neurol Neurosurg Psychiatry. 80 : 366-380, 2009.
3) Kim KW, Park JH, Kim MH, Kim BJ, Kim SK, Kim JL, Moon SW, Bae JN, Woo JI, Ryu SH, Yoon JC, Lee NJ, Lee DY, Lee DW, Lee SB, Lee JJ, Lee JY, Lee CU, Chang CM, Jhoo JH and Cho MJ : A nationwide survey on the prevalence of Dementia and Mild Cognitive Impairment in South Korea. J Alzheimer Dis. 23 : 281-291, 2011.
4) Wallin A, Andreasen N, Eriksson S, Batsman S, Näsman B, Ekdahl A, Kilande L, Grut M, Ryden M, Wallin A, Jonsson M, Olofsson H, Londos E, Wattmo C, Jönhagen M, Minthon L, the Swedish Alzheimer Treatment Study Group : Donepezil in Alzheimer's disease : what to expect after 3

years of treatment in a routine clinical setting. Dement Geriatr Cogn Disord. 23 : 150-160, 2007.
5) Birks J : Cholinesterase inhibitors for Alzheimer's disease (review), In : The Cochrane Library, Issue 1. John Wiley & Sons Ltd. Hoboken, 2009.
6) Wattmo C, Wallin A, Londos E and Minthon L : Long-term outcome and prediction models in activities of daily living in Alzheimer disease with cholinesterase inhibitor treatment. Alzheimer Dis Assoc Disor. 25 : 63-72, 2011.
7) Aisen PS, Andrieu S, Sampaio C, Carrillo M, Khachaturian ZS, Dubois B, Feldman HH, Petersen RC, Siemers E, Doody RS, Hendrix SB, Grundman M, Schneider LS, Schnidler RJ, Salmon E, Potter WZ, Thomas RG, Salmon D, Donohue M, Bednar MM, Touchon J and Vellas B : Report of the task force on designing clinical trials in early (predementia) AD. Neurology. 76 : 280-286, 2011.
8) Ashburner, J and Friston, KJ : Voxel-based morphometry : the methods. Neuroimage. 11 : 805-821, 2000.
9) Testa C, Laakso MP, Sabattoli F, Rossi R, Beltramello A, Soininen H and Frisoni GB : A comparison of accuracy of voxel-based morphometry and hippocampal volumetry in Alzheimer's disease J Magn Reson Imaging. 19 : 274-282, 2004.
10) Ishii K, Kawachi T, Sasaki H, Kono AK, Fukuda T, Kojima Y, Mori E Voxel-based morphometric comparison between early- and late-onset mild Alzheimer's disease and assessment of diagnostic performance of Z score images. AJNR Am J Neuroradiol. 25 : 333-340, 2005.
11) Hirata Y, Matsuda H, Nemoto K, Nemoto K, Ohnishi T, Hirao K, Yamashita F, Asada T, Iwabuchi S and Samejima H : Voxel-based morphometry to discriminate early Alzheimer's disease from controls. Neurosci Lett. 382 : 269-274, 2005.
12) Matsuda H : The role of neuroimaging in mild cognitive impairment. Neuropathology. 27 : 570-577, 2007.
13) McKhann G, Drachman D, Folstein M, Katzman R, Price D and Stadlan M : Clinical diagnosis of Alzheimer's disease : report of the NINCDS-ADRDA Work Group under the auspices of Department of Health and Human Services Task Force on Alzheimer's disease. Neurology. 34 : 939-944, 1984.
14) American Psychiatric Association : Diagnostic and statistical manual of mental disorders : DSM-IV 4th ed. American Psychiatric Association, Washington, 1994.
15) Folstein M, Folstein S and McHugh P : "Mini-Mental State": a practical method for grading the cognitive state of patients for the clinician. J Psychiatr Res. 12 : 189-198, 1975.
16) Román G, Tatemichi T, Erkinjuntti T, Cummings J, Masdeu J, Garcia J, Amaducci L, Orgogozo J, Brun A, Hofman A, Moody D, O'Brien M, Yamaguchi T, Grafman J, Drayer B, Bennett D, Wolf P, Gorelick P, Bick K, Pajeau A, Bell M, Phil D, DeCarli C, Culebras A, Korczyn A, Bogousslavsky J, Hartman A and Scheinberg P : Vascular dementia : diagnostic criteria for research studies. Report of the NINDS-AIREN International Workshop. Neurology. 43 : 250-260, 1993.
17) Zung W : A self-rating depression scale. Arch Gen Psychiatry. 12 : 63-70, 1965.
18) Ashburner J : A fast diffeomorphic image registration algorithm. NeuroImage. 38 : 95-113, 2007.
19) Good CD, Johnsrude IS, Ashburner J, Henson RNA, Friston KJ, Frackowiak SJ. A voxel-based morphometric study of ageing in 465 normal adult human brains. NeuroImage. 14 : 21-36, 2001.
20) Jack Jr C, Petersen RC, Xu YC, Waring S, O'Brien P, Tangalos E, Smith G, Ivnik R and Kokmen E : Medial temporal atrophy on MRI in normal aging and very mild Alzheimer's disease. Neurology. 49 : 786-794, 1997.
21) Karas G, Burton E, Rombouts S, van Schinjdel R, O'Brien J, Scheltens P, McKeith I, Williams D, Ballard C and Barkhof F : A comprehensive study of gray matter loss in patients with Alzheimer's disease using optimized voxel-based morphometry. NeuroImage. 18 : 895-907, 2003.
22) Chetelat G and Baron J : Early diagnosis of Alzheimer's disease : contribution of structural neuroimaging. NeuroImage. 18 : 525-541, 2003.
23) Thompson P, Hayashi K, Zubicaray G, Janke A, Rose S, Semple J, Herman D, Hong M, Dittmer S, Doddrell D and Toga A : Dynamics of gray matter loss in Alzheimer`s disease. J Neurosci. 23 : 994-1005, 2003.
24) Frisoni G, Testa C, Zorzan A, Sabattoli F, Beltramello A, Soininen H and Laakso M : Detection of grey matter loss in mild Alzheimer's disease with voxel based morphometry. Ashburner J : A fast diffeomorphic image registration algorithm. NeuroImage. 38 : 95-113, 2007.

25) Apostolova L, Steiner C, Akopyan G, Dutton R, Hayashi K, Toga A, Cummings J and Thomson P : Three-dimensional gray matter atrophy mapping in mild cognitive impairment and mild Alzheimer disease. Arch Neurol. 64 : 1489-1495, 2007.
26) Dickerson B, Feczko E, Augustinack J, Pacheco J, Morris J, Fischl B and Buckner R : Differential effects of aging and Alzheimer's disease on medial temporal lobe cortical thickness and surface area. Neurobiol Aging. 30 : 432-440, 2009.
27) Brun A and Englund E : Regional pattern of degeneration in Alzheimer's disease : neuronal loss and histopathological grading. Histopathology. 5 : 549-564, 1981.
28) Braak H and Braak E : Neuropathological staging of Alzheimer-related changes. Acta Neuropathol. 82 : 239-259, 1991.
29) Hyman B : The neuropathological diagnosis of Alzheimer's disease : clinical-pathological studies. Neurobiology of Aging. 18 : 27-32, 1997.
30) Wilke M, Kassubek J, Ziyeh S, Schulze-Bonhage A and Huppertz H : Automated detection of gray matter malformations using optimized voxel-based morphometry : a systematic approach. NeuroImage. 20 : 330-343, 2003.
31) Mak AKY, Wong M, Han S and Lee TMC : Gray matter reduction associated with emotion regulation in female outpatients with major depressive disorder : a voxel-based morphometry study. Prog Neuropsychopharmacol Biol Psych. 33 : 1184-1190, 2009.
32) Bruggermann J, Wilke M, Som S, Bye A, Bleasel A and Lawson J : Voxel-based morphometry in the detection of dysplasia and neoplasia in childhood epilepsy : limitations of GM analysis. J Clin Neurosci. 16 : 780-785, 2009.
33) Fortino A, Yücel M, Patti J, Wood S and Pantelis C : Mapping of grey matter reduction in schizophrenia : an anatomical likelihood estimation analysis of voxel-based morphometry studies. Schizophrenia Research. 108 : 104-113, 2009.
34) Matsunari I, Samuraki M, Chen W-P, Yanase D, Takeda N, Ono K, Yoshita M, Matsuda H, Yamada M and Kinuya S : Comparison of 18F-FDG PET and optimized voxel-based morphometry for detection of Alzheimer's disease : aging effect on diagnostic performance. J Nucl Med. 48 : 1961-1970, 2007.
35) Klein A, Andersson J, Ardekani BA, Ashburner J, Avants B, Chiang M-C, Christensen GE, Collins DL, Gee J, Hellier P, Song JH, Jenkinson M, Lepage C, Rueckert D, Thompson P, Vercauteren T, Woods RP, Mann JJ and Parsey RV : Evaluation of 14 nonlinear deformation algorithms applied to human brain MRI registration. Neuroimage. 46 : 786-802, 2009.

(Received for publication August 22, 2011)

（和文抄録）

Voxel-Based Morphometry に基づく Alzheimer 病の診断：解析法の影響

[1)] 九州大学大学院医学研究院 臨床放射線科学分野
[2)] 九州大学大学院医学研究院 神経内科学分野
[3)] 九州大学大学院医学研究院 精神病態医学分野

Tuvshinjargal Dashjamts[1)]，吉浦　敬[1)]，樋渡昭雄[1)]，栂尾　理[1)]，山下孝二[1)]，大八木保政[2)]，門司　晃[3)]，鎌野宏礼[1)]，川島敏郎[3)]，吉良潤一[2)]，本田　浩[1)]

目的：voxel-based morphometry（VBM）による脳形態解析に基づく Alzheimer 病患者と健常者の判別における，最適な解析法を明らかにすることが目的である．
対象と方法：24 名の Alzheimer 病患者と 26 名の健常者を対象とした．それぞれの被験者の脳 T1 強調 MR 画像を VBM の手法に従って解析し，Alzheimer 病による有意な灰白質減少を示す脳領域を求めた．VBM 解析は，modulation を行わない灰白質濃度の解析と，modulation を行うことで得られる灰白質体積の解析の両者を，それぞれ全脳による正規化（global normalization）を加えて行う場合と加えずに行う場合の，計 4 種類の解析法で行った．それぞれの方法において，３段階の P 値設定（$P < 0.001$，$P < 0.0005$ および $P < 0.0001$）で statistical parametric mapping 解析を行い，得られた有意な灰白質減少を示す脳領域内での平均灰白質濃度または体積に基づいて，患者と健常者の判別を行った．receiver operating characteristic 解析と判別分析を用いて，異なる方法の間で判別能の比較を行った．
結果：灰白質濃度による解析は，灰白質体積による解析に比較して，判別能が高かった．global normalization の有無の影響は明らかではなかった．
結論：VBM に基づく Alzheimer 病患者と健常者の判別には，灰白質体積による解析よりも灰白質濃度による解析が適していると考えられた．